

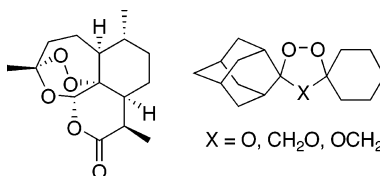
Dispiro-1,2,4-trioxane Analogues of a Prototype
Dispiro-1,2,4-trioxolane: Mechanistic Comparators for Artemisinin
in the Context of Reaction Pathways with Iron(II)

Yuanqing Tang,[†] Yuxiang Dong,[†] Xiaofang Wang,[†] Kamaraj Sriraghavan,[†]
James K. Wood,[‡] and Jonathan L. Vennerstrom^{*,†}

College of Pharmacy, University of Nebraska Medical Center, 986025 Nebraska Medical Center,
Omaha, Nebraska 68198-6025, and Department of Chemistry, University of Nebraska at Omaha,
60th and Dodge Street, Omaha, Nebraska 68192-0109

jvenners@unmc.edu

Received March 1, 2005



Single electron reduction of the 1,2,4-trioxane heterocycle of artemisinin (**1**) forms primary and secondary carbon-centered radicals. The complex structure of **1** does not lend itself to a satisfactory dissection of the electronic and steric effects that influence the formation and subsequent reaction of these carbon-centered free radicals. To help demarcate these effects, we characterized the reactions of achiral dispiro-1,2,4-trioxolane **4** and dispiro-1,2,4-trioxanes **5–7** with ferrous bromide and 4-oxo-TEMPO. Our results suggest a small preference for attack of Fe(II) on the nonketal peroxide oxygen atom of **1**. For **4**, but not for **5** and **6**, there was a strong preference for attack of Fe(II) on the less hindered peroxide bond oxygen atom. The steric hindrance afforded by a spiroadamantane in a five-membered trioxolane is evidently much greater than that for a corresponding six-membered trioxane. Unlike **1**, **5–7** fragment by entropically favored β -scission pathways forming relatively stable α -oxa carbon-centered radicals. These data suggest that formation of either primary or secondary carbon-centered radicals is a necessary but insufficient criterion for antimalarial activity of **1** and synthetic peroxides.

Introduction

Artemisinin and Iron(II). The discovery of artemisinin (**1**, qinghaosu) and its semisynthetic derivatives provided a new class of antimalarial drugs. As summarized by Klayman,¹ early work demonstrated that the pharmacophoric peroxide bond in the 1,2,4-trioxane heterocycle of **1** is essential for activity. Considerable evidence² suggests that the peroxide bond in **1** undergoes reductive activation by heme released by parasite hemoglobin digestion. This irreversible redox reaction produces

carbon-centered free radicals³ or carbocations⁴ that may convey the parasiticidal effects and unique antimalarial specificity of the artemisinins by alkylation of heme⁵ or proteins,⁶ including the putative target SERCA PfATP6.⁷ The two major pathways (Scheme 1) for reductive cleavage of **1**⁸ are initiated by delivery of an electron from

* To whom correspondence should be addressed. Tel: 402.559.5362. Fax: 402.559.9543.

[†] University of Nebraska Medical Center.

[‡] University of Nebraska at Omaha.

(1) Klayman, D. L. *Science* **1985**, *228*, 1049–1055.

(2) (a) Robert, A.; Meunier, B. *Chem. Soc. Rev.* **1998**, *27*, 273–279. (b) Jefford, C. W. *Curr. Med. Chem.* **2001**, *8*, 1803–1826. (c) Dong, Y.; Vennerstrom, J. L. *Redox Rep.* **2003**, *8*, 284–288. (d) Posner, G. H.; O'Neill, P. H. *Acc. Chem. Res.* **2004**, *37*, 397–404. (e) O'Neill, P. M.; Posner, G. H. *J. Med. Chem.* **2004**, *47*, 2945–2964.

(3) Butler, A. R.; Gilbert, B. C.; Hulme, P.; Irvine, L. R.; Renton, L.; Whitwood, A. C. *Free Rad. Res.* **1998**, *28*, 471–476.

(4) Szpilman, A. M.; Korshin, E. E.; Hoos, R.; Posner, G. H.; Bachi, M. D. *J. Org. Chem.* **2001**, *66*, 6531–6540.

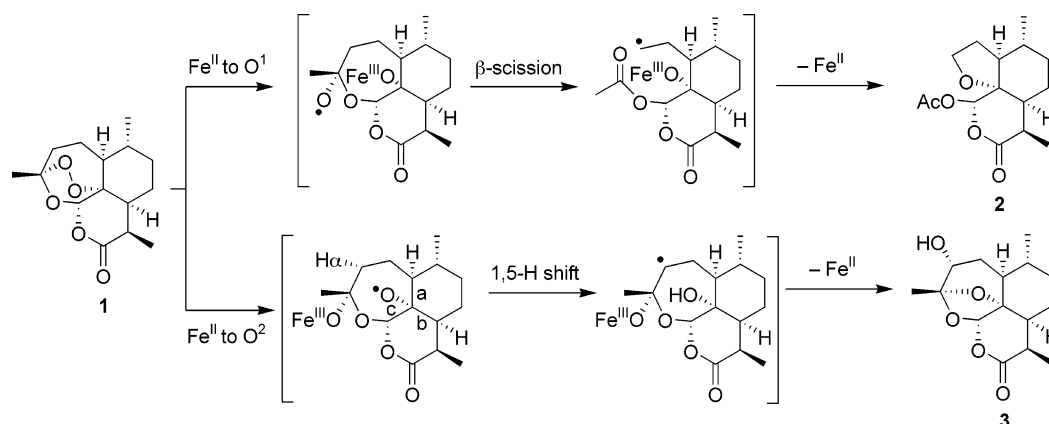
(5) Robert, A.; Coppel, Y.; Meunier, B. *Chem. Commun.* **2002**, 414–415.

(6) Meshnick, S. R. Artemisinin: Mechanisms of Action, Resistance and Toxicity. *Int. J. Parasitol.* **2002**, *32*, 1655–1660.

(7) Eckstein-Ludwig, U.; Webb, R. J.; van Goethem, I. D. A.; East, J. M.; Lee, A. G.; Kimura, M.; O'Neill, P. M.; Bray, P. G.; Ward, S. A.; Krishna, S. *Nature* **2003**, *424*, 957–961.

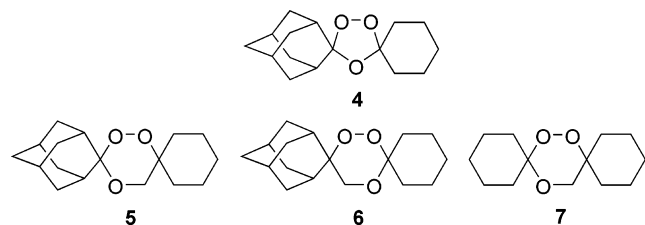
(8) (a) Posner, G. H.; Oh, C. H. *J. Am. Chem. Soc.* **1992**, *114*, 8328–8329. (b) Jefford, C. W.; Vicente, M. G. H.; Jacquier, Y.; Favarger, F.; Mareda, J.; Millasson-Schmidt, P.; Brunner, G.; Burger, U. *Helv. Chim. Acta* **1996**, *79*, 1475–1487. (c) Gu, J.; Chen, K.; Jiang, H.; Leszczynski, J. *J. Phys. Chem. A* **1999**, *103*, 9364–9369.

SCHEME 1



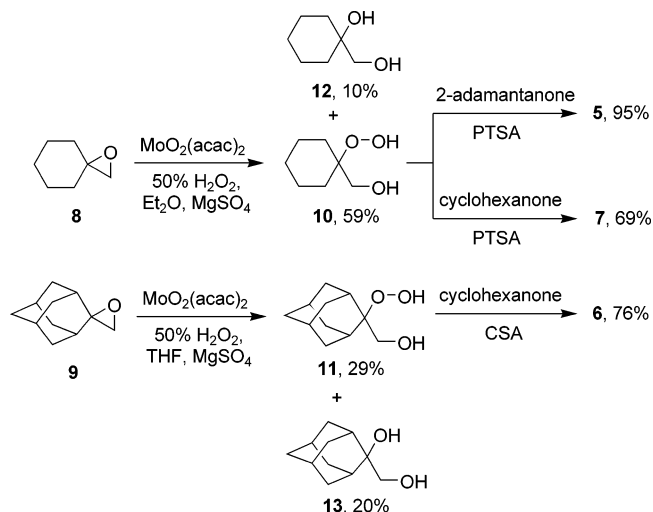
Fe(II) to the antibonding σ^* orbital of the peroxide bond to form a pair of oxy radicals. The first involves the attack of Fe(II) on O¹ of the peroxide bond, producing an O² free radical. This oxygen free radical is short-lived and rearranges via β -scission to a C4-centered primary radical thermodynamically facilitated by concomitant formation of an ester functionality; apparently, no methyl radical is produced by the alternate β -scission pathway. In the second, initial attack of Fe(II) on O² of the peroxide linkage results in formation of an O¹ free radical. Rather than fragment by any of the three possible β -scission pathways a–c, the O¹ free radical undergoes a 1,5 H-shift, giving rise to a C4-centered secondary radical. Both artemisinin-derived C4-centered radicals are irreversibly formed kinetic intermediates^{2b} that self-quench⁹ in intramolecular reactions to produce **2** and **3**, both of which are devoid of antimalarial activity. In summary, available evidence suggests that electron transfer leading to formation of carbon-centered radicals may constitute the required activation step of the artemisinins and other peroxidic antimalarials.

Whether the primary or secondary carbon-centered radicals or a combination of the two contribute to the antimalarial activity of **1** has been a subject of debate. The difficulty lies in the fact that both carbon-centered radicals can be observed in iron(II) models, largely depending on the particular reaction conditions, including solvents and counterions as discussed in detail by Wu et al.¹⁰ The complex structure of **1** does not lend itself to satisfactory dissection of the electronic and steric effects that influence the formation and subsequent reaction of these carbon-centered free radicals. On the basis of the achiral prototype dispiro-1,2,4-trioxolane **4**,¹¹ we envisioned that achiral dispiro-1,2,4-trioxanes **5–7** could provide tools to help demarcate these effects.



(9) Wu, Y. *Acc. Chem. Res.* **2002**, *35*, 255–259.

SCHEME 2. Synthesis of 5–7



Results and Discussion

Trioxane Synthesis. Preparation of target trioxanes **5–7** (Scheme 2) required precursor β -hydroperoxy alcohols **10** and **11**. Although β -hydroperoxy alcohols have been prepared by treatment of epoxides with anhydrous H₂O₂ with^{12,13} or without¹⁴ an acid catalyst, we elected to use the commercially available 50% aqueous H₂O₂ as a safer alternative. Hydroperoxidation of spiro epoxide **8**¹⁵ with 50% aqueous H₂O₂ (10 equiv) pretreated with anhydrous MgSO₄ (ca. 1 g of anhydrous MgSO₄ per 1 mL of 50% H₂O₂ in 15 mL of ether) and molybdenyl acetylacetonate (5%)¹⁶ as catalyst afforded **10**¹² in modest yield.

(10) Wu, W. M.; Wu, Y.; Wu, Y.-L.; Yao, Z.-J.; Zhou, C.-M.; Li, Y.; Shan, F. *J. Am. Chem. Soc.* **1998**, *120*, 3316–3325.

(11) Vennerstrom, J. L.; Arbe-Barnes, S.; Brun, R.; Charman, S. A.; Chiu, F. C. K.; Chollet, J.; Dong, Y.; Dorn, A.; Hunziker, D.; Matile, H.; McIntosh, K.; Padmanilayam, M.; Santo Tomas, J.; Scheurer, C.; Scorneaux, B.; Tang, Y.; Urwyler, H.; Wittlin, S.; Charman, W. N. *Nature* **2004**, *430*, 900–904.

(12) Kerr, B.; McCullough, K. *J. Chem. Soc., Chem. Commun.* **1985**, 590–592.

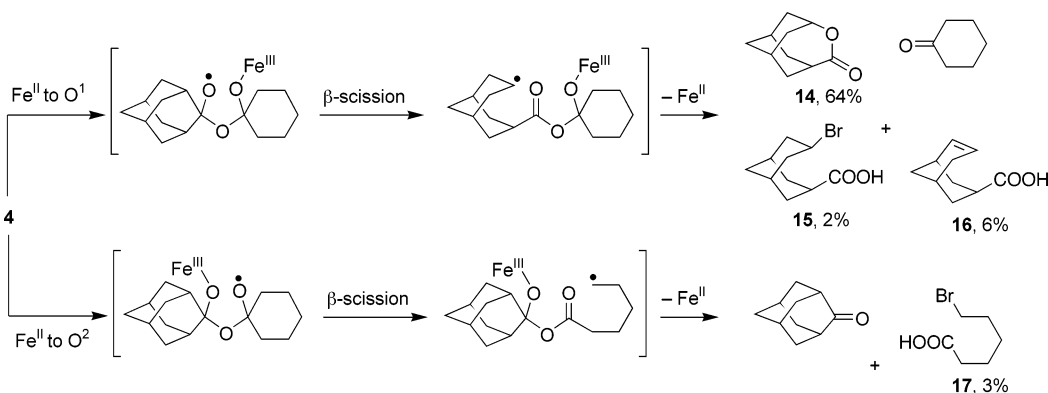
(13) Subramanyam, V.; Brizuela, C. L.; Soloway, A. H. *J. Chem. Soc. Chem. Commun.* **1976**, 508–509.

(14) Adam, W.; Peters, K.; Renz, M. *J. Org. Chem.* **1997**, *62*, 3183–3189.

(15) (a) Corey, E. J.; Chaykovsky, M. *J. Am. Chem. Soc.* **1962**, *84*, 3782–3783. (b) Johnson, C. R.; Mori, K.; Nakanishi, A. *J. Org. Chem.* **1979**, *44*, 2065–2067.

(16) Mattucci, A. M.; Perrotti, E.; Santambrogio, A. *J. Chem. Soc., Chem. Commun.* **1970**, 1198–1199.

SCHEME 3



Use of alternative solvents and catalysts such as THF and sulfuric acid, respectively, led to decreased ratios of **10** and diol **12**¹⁷ and lower reaction yields. Under nearly identical conditions, hydroperoxidation of spiro epoxide **9**¹⁸ afforded **11** in low yield accompanied by nearly equal quantities of diol **13**.¹⁹ Little or no conversion of **9** to **11** took place using other solvents (ether, acetonitrile, 2-propanol) or catalysts.

In the presence of catalytic *p*-toluenesulfonic acid (PTSA), target trioxanes **5** and **7**^{20,21} were readily formed by reaction of **10** with 2-adamantanone and cyclohexanone, respectively. Similarly, reaction of **11** with cyclohexanone in the presence of catalytic camphorsulfonic acid (CSA) afforded target trioxane **6**. Trioxane **5** was also obtained (77% yield) using the triethylsilylperoxy derivative of **10**, although the latter was obtained in yields of less than 30% from 1-cyclohexene-1-methanol using the method of O'Neill et al.^{21a} (data not shown).

Antimalarial Activity. The antimalarial properties of **5–7** compared to that of **1** and **4** were measured against *P. falciparum* in vitro and *P. berghei* in vivo.²² The results were unexpected in that **5** and **7** with IC₅₀'s of 49 and 120 ng/mL were an order of magnitude less potent than **1** and **4** (IC₅₀'s of 1.6 and 1.2 ng/mL). Trioxane **6** (IC₅₀ > 1000 ng/mL) was inactive against *P. falciparum* in vitro. Furthermore, each of the trioxanes was completely inactive against *P. berghei* when they were administered at 100 mg/kg oral and subcutaneous doses on day 1 postinfection; in contrast **1** and **4** had oral ED₅₀/ED₉₀'s of 9.1/14 and 4.0/8.8 mg/kg.

Reactions with Iron(II). Next, we turned our attention to investigating the reaction pathways of **4–7** with FeBr₂ (1 equiv) in THF^{8a} not only to shed further light

on the mechanism of action of **1** but also to understand the striking loss of antimalarial activity of **5** and **6** compared to that of **1** and **4**.

Reaction of **4** with iron(II) produced lactone **14**, bromoacid **15** and unsaturated acid **16**²³ in a combined isolated yield of 72% along with a 3% yield of 6-bromohexanoic acid **17**²⁴ (Scheme 3). This result was confirmed by the 22:1 ratio of cyclohexanone and 2-adamantanone trapped as their oxime ethers²⁵ by post-reaction treatment with *O*-benzylhydroxylamine and pyridine and quantitated by ¹H NMR.²⁶ The 22–24:1 ratio of reaction products resulting from β-scission of the spiroadamantane and spirocyclohexanone, respectively, indicates regioselective formation of the oxy radical resulting from preferential attack of Fe(II) on the less hindered peroxide bond oxygen atom (O¹) of **4**. Similar regioselective iron-mediated decompositions of other unsymmetrical trioxanes due to steric hindrance were noted by Abe et al.²⁷

Reaction of **5** with iron(II) produced bromoester carbinols **18** and **19**, unsaturated ester carbinol **20**, 2-adamantanone, cyclohexanone, and formaldehyde (Scheme 4). A 2:1 ratio of the O¹:O² pathways was evident in the 2:1:1:0.43 ratio of (**18** + **20**)/2-adamantanone/cyclohexanone/formaldehyde, the latter three of which were quantitated²⁶ as their *O*-benzyl oximes.^{25,28} The less than theoretical quantity of formaldehyde observed was probably due to the loss of formaldehyde during the reaction and of its *O*-benzyl oxime during the reaction workup.²⁹ Bromoester carbinol **18** was initially formed as a 2:1 mixture of two isomers that isomerized both in the crude reaction mixture and in CDCl₃ solution to form a mixture of four isomers. These four 3,7-disubstituted bicyclo[3.3.1]nonane isomers could be purified to 80–95% by RP-HPLC, but their exo/endo stereochemistry was not

(17) Itami, K.; Kamei, T.; Mitsudo, K.; Nokami, T.; Yoshida, J.-I. *J. Org. Chem.* **2001**, *66*, 3970–3976.

(18) Olah, G. A.; Wu, A.-H. *Synthesis* **1990**, 887–889.

(19) Farcasiu, D.; Schleyer, P. V. R.; Ledlie, D. B. *J. Org. Chem.* **1973**, *38*, 3455–3459.

(20) Haq, A.; Kerr, B.; McCullough, K. J. *J. Chem. Soc., Chem. Commun.* **1993**, 1076–1078.

(21) (a) O'Neill, P. M.; Hindley, S.; Pugh, M. D.; Davies, J.; Bray, P. G.; Park, B. K.; Kapu, D. S.; Ward, S. A.; Stocks, P. A. *Tetrahedron Lett.* **2003**, *44*, 8135–8138. (b) Ahmed, A.; Dussault, P. H. *Org. Lett.* **2004**, *6*, 3609–3611. In this paper, the same Co(thd)₂ catalyst is employed as the method of choice for hydroperoxysilylation.

(22) In vitro activity was measured against the chloroquine-sensitive NF54 (airport, unknown origin) and chloroquine-resistant KI (Thailand) strains of *Plasmodium falciparum*. The IC₅₀'s are average values (*n* = 2 to 3) against the NF54 and KI strains. In vivo activity was measured against *P. berghei* as previously described (ref 11). Against the KI strain, O'Neill et al. (ref 21) report an IC₅₀ of 33 ng/mL for **7**; our measured IC₅₀ of 130 ng/mL for **7** was 4-fold higher.

(23) Bridges, A. J.; Raman, P. S.; Ng, G. S. Y.; Jones, J. B. *J. Am. Chem. Soc.* **1984**, *106*, 1461–1467.

(24) McGrady, J.; Laughlin, R. G. *Synthesis* **1984**, 426–428.

(25) Bhat, J. I.; Clegg, W.; Maskill, H.; Elsegood, M. R. J.; Menneer, I. D.; Miatt, P. C. *J. Chem. Soc., Perkin Trans. 2* **2000**, 1435–1446.

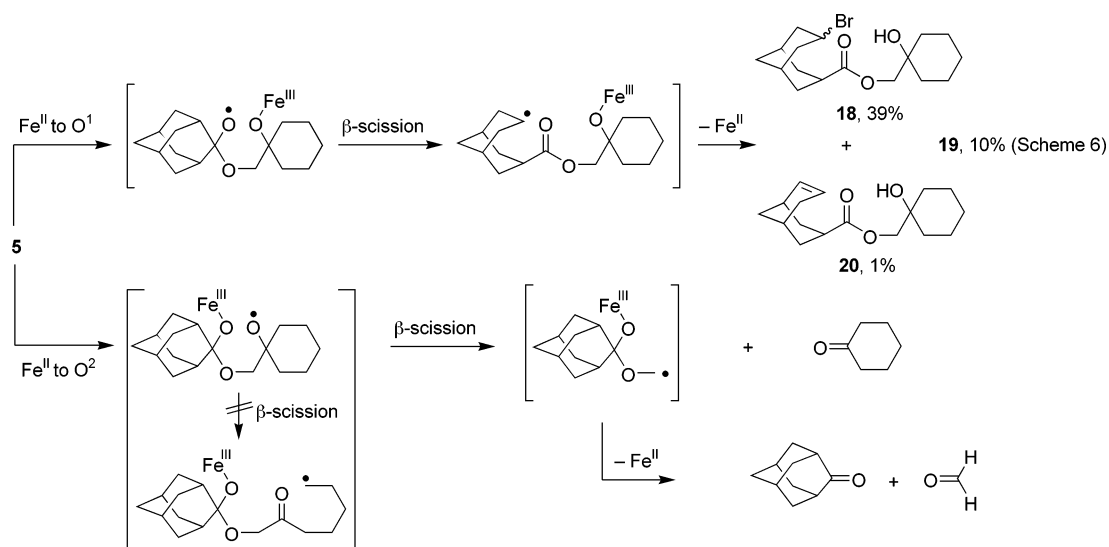
(26) Because of the volatility of 2-adamantanone, cyclohexanone, and formaldehyde, their less volatile *O*-benzyl oximes (refs 25 and 28) were independently prepared to identify diagnostic ¹H NMR signals appropriate for quantitation: δ 3.57 (s), 2.20 (t), and 7.08 (d), respectively.

(27) Abe, M.; Inakazu, T.; Munakata, J.; Nojima, M. *J. Am. Chem. Soc.* **1999**, *121*, 6556–6562.

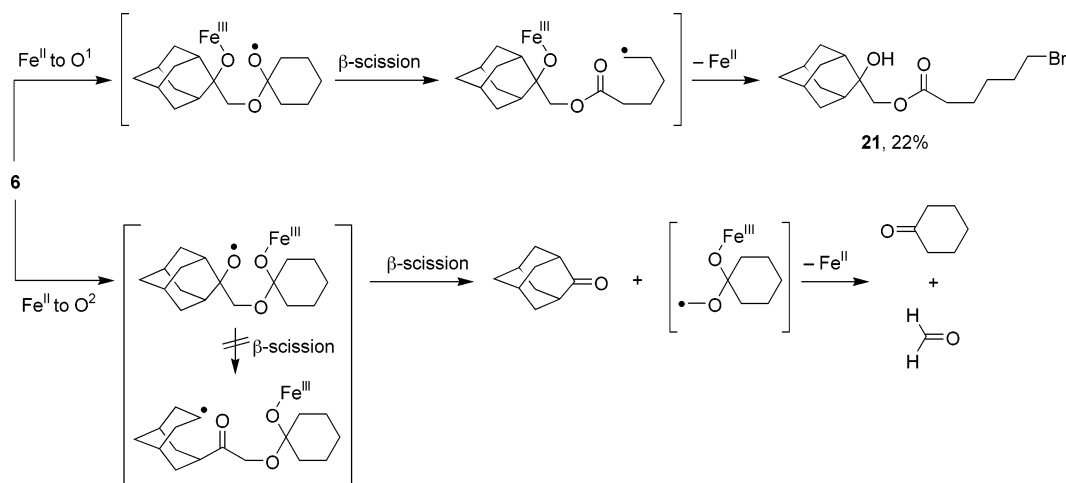
(28) Hart, D. J.; Seely, F. L. *J. Am. Chem. Soc.* **1988**, *110*, 1631–1633.

(29) For **5–7**, we also observed small quantities of benzaldehyde *O*-benzyl oxime (δ 8.14) (ref 25) that may have arisen from Fe(III) oxidation of *O*-benzylhydroxylamine to form benzaldehyde that subsequently reacted with *O*-benzylhydroxylamine.

SCHEME 4



SCHEME 5



defined³⁰ because of difficulty in calculating coupling constants, although exo 7-bromo and 3-ester substituents in one (**18d**) of the isomers were deduced by a strong correlation between H-3 (2.82–2.91 ppm) and H-7 (4.68–4.76 ppm) in the NOESY spectrum. The only way we could account for the formation of bromoester carbinol **19** (vide infra; Scheme 6) was via iron(II) decomposition of trioxane **7** formed from cyclohexanone and β-hydroperoxy alcohol **10** liberated during the course of the reaction of **5** with iron(II). An analogous Lewis acid catalyzed heterolytic fragmentation of the 1,2,4-trioxane ring of artemisinin has been previously proposed.³¹

This 2:1 proportion of reaction products indicates a modest preference for attack of Fe(II) on the less hindered peroxide bond oxygen atom (O¹) of **5**. Interestingly, attack of Fe(II) on the more hindered peroxide bond oxygen atom (O²) generates an Fe(III)-complexed oxy radical that can undergo two β-scission pathways, only one of which is

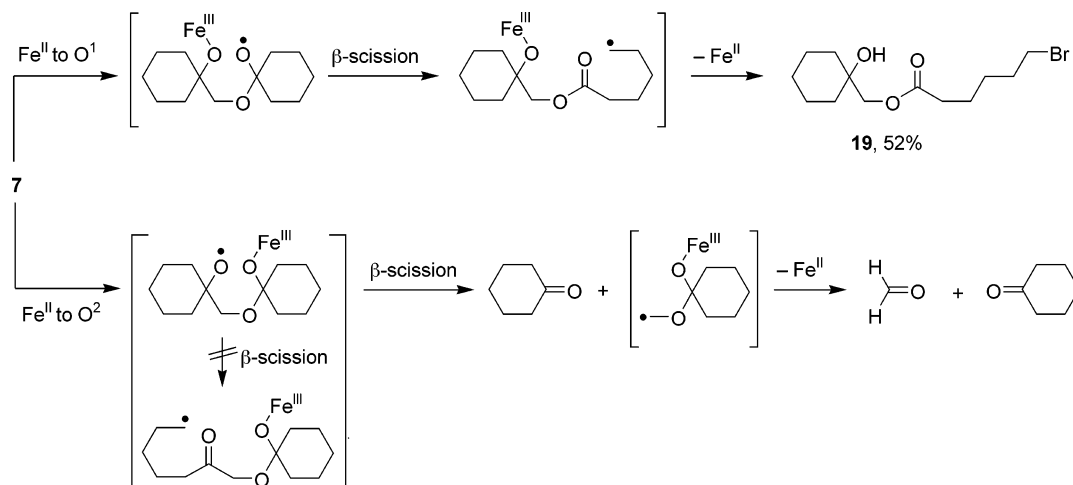
observed. In this pathway, an α-oxa primary carbon-centered radical and cyclohexanone are initially formed, and the former then unravels to 2-adamantanone and formaldehyde. We observed no α-hydroxy ketone reaction product that would have arisen from the β-scission pathway to form the primary carbon-centered radical.

Reaction of **6** with iron(II) produced bromoester carbinol **21**, 2-adamantanone, cyclohexanone, and formaldehyde (Scheme 5). A 1:3 ratio of the O¹:O² pathways was evident in the 1:3:1.3:3:1.5 ratio of **21**/2-adamantanone/cyclohexanone/formaldehyde, the latter three of which were quantitated²⁶ as their *O*-benzyl oximes.^{25,28} As was the case for **5**, the less than theoretical quantity of formaldehyde observed was probably due to the loss of formaldehyde during the reaction and of its *O*-benzyl oxime during the reaction workup. This 1:3 proportion of reaction products indicates a modest preference for attack of Fe(II) on the less hindered peroxide bond oxygen atom (O²) of **6**. Attack of Fe(II) on O² generates an Fe(III) complexed oxy radical that can undergo two β-scission pathways, only one of which is observed. In this pathway, 2-adamantanone and an α-oxa primary carbon-centered radical are initially formed, and the latter then unravels

(30) (a) Peters, J. A.; Van Der Toorn, J. M.; Van Bekkum, H. *Tetrahedron* **1975**, *31*, 2273–2281. (b) Peters, J. A.; van Ballegoyen-Eekhout, G. W. M.; van de Graaf, B.; Bovée, W. M. M. J.; Baas, J. M. A.; van Bekkum H. *Tetrahedron* **1983**, *39*, 1649–1654.

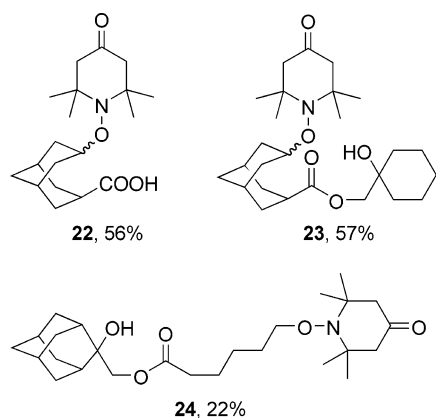
(31) Haynes, R. K.; Pai, H. H. O.; Voerste, A. *Tetrahedron Lett.* **1999**, *40*, 4715–4718.

SCHEME 6



to cyclohexanone and formaldehyde. Similar to **5**, we observed no α -hydroxy ketone reaction product that would have arisen from the β -scission pathway to form the secondary carbon-centered radical.

For **4**–**6**, confirmation of the proposed carbon-centered free radical intermediates was provided by spin-trapping experiments with the nitroxide free radical, 4-oxo-2,2,6,6-tetramethyl-1-piperidinyl-oxo (4-oxo-TEMPO). Treatment of **4** with 1.5 equiv each of FeBr_2 and 4-oxo-TEMPO in THF did form the expected aminoxy acid **22** in 7% yield, but the major product was **14** (70%) accompanied by **15** (8%), **16** (3%), and **17** (6%). However, using conditions (1.5 equiv of $\text{Fe}(\text{OAc})_2$ and 2 equiv of 4-oxo-TEMPO in 1:1 $\text{CH}_2\text{Cl}_2/\text{CH}_3\text{CN}$) that we had used earlier in a similar experiment¹¹ with a trioxolane ketone, **22** was produced in 56% yield along with **14** (28%) and **16** (6%). For **5** and **6**, reactions were conducted with 2.5 equiv each of FeBr_2 and 4-oxo-TEMPO in THF. Trioxane **5** formed aminoxy ester alcohol **23** (57%), 2-adamantanone (3%), and unsaturated ester carbinol **20** (4%). Trioxane **6** formed aminoxy ester alcohol **24** (22%) and 2-adamantanone (39%). Aminoxy reaction products **22**–**24** correspond to the proposed carbon-centered free radical intermediates invoked to account for the observed reaction products in Schemes 3–5. However, this does not necessarily imply that bromoacids **15** and **17**, bromoester carbinols **18**, **19** (Scheme 6; *vide infra*), and **21**, the unsaturated acid **16** and ester carbinol **20** were formed exclusively by carbon-centered radical pathways. For example, an alternative mechanism to account for the formation of **15**–**21** is



intra- or intermolecular electron transfer between Fe(III) and the carbon-centered radicals to simultaneously regenerate Fe(II) and produce the corresponding carbocations,^{2b,4} the latter of which could react with bromide or undergo elimination.

Reaction of **7** with iron(II) produced bromoester carbinol **19**, cyclohexanone, and formaldehyde (Scheme 6). A 1:1.4 ratio of **19**:cyclohexanone was observed; the latter was quantitated²⁶ as its *O*-benzyl oxime.²⁵ Since the O^2 pathway produces 2 equiv of cyclohexanone, this result indicates a 3:2 ratio of the O^1 : O^2 pathways. Since steric effects do not play a role in reaction of **7** with iron(II), this proportion of reaction products indicates a small preference for attack of Fe(II) on the nonketal peroxide oxygen atom (O^1) of the peroxide bond. In this pathway, subsequent β -scission simultaneously forms a primary carbon-centered radical and ester. Attack of Fe(II) on O^2 generates an Fe(III) complexed oxy radical that can undergo two β -scission pathways, only one of which is observed. In this pathway, cyclohexanone and an α -oxa primary carbon-centered radical are initially formed, and the latter then unravels to formaldehyde and a second molecule of cyclohexanone. As was observed for **5** and **6**, such entropically favored O^2 β -scission reaction pathways that form relatively stable³² α -oxa primary carbon-centered radicals are apparently much too rapid to observe the competing β -scission pathways³³ leading to the unobserved α -hydroxy ketone reaction products. Similar α -oxa carbon-centered radicals may be invoked to account for the carbonyl end products produced from single-electron reductions of other synthetic trioxanes.³⁴

Discussion. We suggest that the observed reaction product distributions in the reactions of **4**–**7** with Fe(II)

(32) Henry, D. J.; Parkinson, C. J.; Mayer, P. M.; Radom, L. *J. Phys. Chem. A* **2001**, *105*, 6750–6756.

(33) Bietti, M.; Lanzalunga, O.; Salamone, M. *J. Org. Chem.* **2005**, *70*, 1417–1422.

(34) (a) Fujisaka, T.; Miura, M.; Nojima, M.; Kusabayashi, S. *J. Chem. Soc., Perkin Trans. 1* **1989**, 1031–1039. (b) Posner, G. H.; Park, S. B.; González, L.; Wang, D.; Cumming, J. N.; Klinedinst, D.; Shapiro, T. A.; Bachi, M. D. *J. Am. Chem. Soc.* **1996**, *118*, 3537–3538. (c) O'Neill, P. M.; Mukhtar, A.; Ward, S. A.; Bickley, J. F.; Davies, J.; Bachi, M. D.; Stocks, P. A. *Org. Lett.* **2004**, *6*, 3035–3038. (d) Provot, O.; Camuzat-Dedenis, B.; Hamzaoui, M.; Moskowit, H.; Mayrargue, J.; Robert, A.; Cazelles, J.; Meunier, B.; Zouhiri, F.; Desmaële, D.; d'Angelo, J.; Mahuteau, J.; Gay, F.; Cicéron, L. *Eur. J. Org. Chem.* **1999**, 1935–1938.

are determined by regioselective formation of one of two possible oxy radicals generated by delivery of an electron from Fe(II) to the peroxide bond antibonding σ^* orbitals²⁷ rather than the relative stability of the two oxy radical species per se. As is observed for **1**,^{2b} the ensuing conversions of the oxy radicals to the more stable^{8c} carbon-centered radical intermediates by β -scission pathways³⁵ are irreversible and strongly exothermic. For **5–7**, the observed reaction products also confirm^{12,20} that ring-opening β -scissions arising from oxy radicals at ketal (O^2) positions occur much faster than competing ring-opening β -scissions arising from oxy radicals at nonketal (O^1) positions.

In consideration of the small preference for attack of Fe(II) on the nonketal peroxide oxygen atom (O^1) of the peroxide bond in **7**, we observed a less than expected 2:1 preference for attack of Fe(II) on the nonketal and sterically less-hindered oxygen atom (O^1) of the peroxide bond in **5** keeping in mind the 3:1 preference for attack of Fe(II) on the ketal and sterically less-hindered oxygen atom (O^2) of the peroxide bond in **6**. For **4** on the other hand, there is a strong preference for attack of Fe(II) on the less hindered peroxide bond oxygen atom (O^1). Since there is little difference in the electronic character of the peroxide oxygen atoms in **4**, apparently steric hindrance to attack of Fe(II) on the more hindered peroxide bond oxygen atom (O^2) determines the observed regioselectivity. In the subsequent reaction pathways, both β -scission pathways are equally facilitated by concomitant ester formation. The regioselectivity of attack of Fe(II) on the peroxide bond afforded by the spiroadamantane in the five-membered 1,2,4-trioxolane **4** is evidently much greater than that for the six-membered 1,2,4-trioxanes **5** and **6**. This is illustrated by the greater steric crowding on the adamantane side of the peroxide bond antibonding σ^* orbital in **4** vs **5** and **6** (Figure 1).

Although conformers of **4–6**³⁶ with the axial peroxide are more stable ($\Delta E = E_{eq} - E_{ax} = 0.280, 1.45, \text{ and } 0.145$ kcal/mol for **4**, **5**, and **6**), conformers with the equatorial peroxide (depicted in Figure 1) provide less steric hindrance to the peroxide antibonding σ^* orbital. As viewed down the axis of the O–O bond of **4**, the σ^* (LUMO) is not visible to the incoming Fe(II) from the adamantane side but is clearly visible and presumably readily accessible to the incoming Fe(II) from the cyclohexane side. For **5** and **6**, the LUMO is not as accessible from either direction as it is from the cyclohexane side of **4**. The reduced accessibility of the LUMO in **5** and **6** is due to the additional methylene group of the trioxane heterocycle increasing the steric hindrance of the peroxide bond by both ring systems. This increased steric effect is manifested by a decrease in the angle between the adamantane and cyclohexane rings as measured through the axis of the peroxide bond. By defining planes of the spiro and vicinal carbon atoms, the angle between the

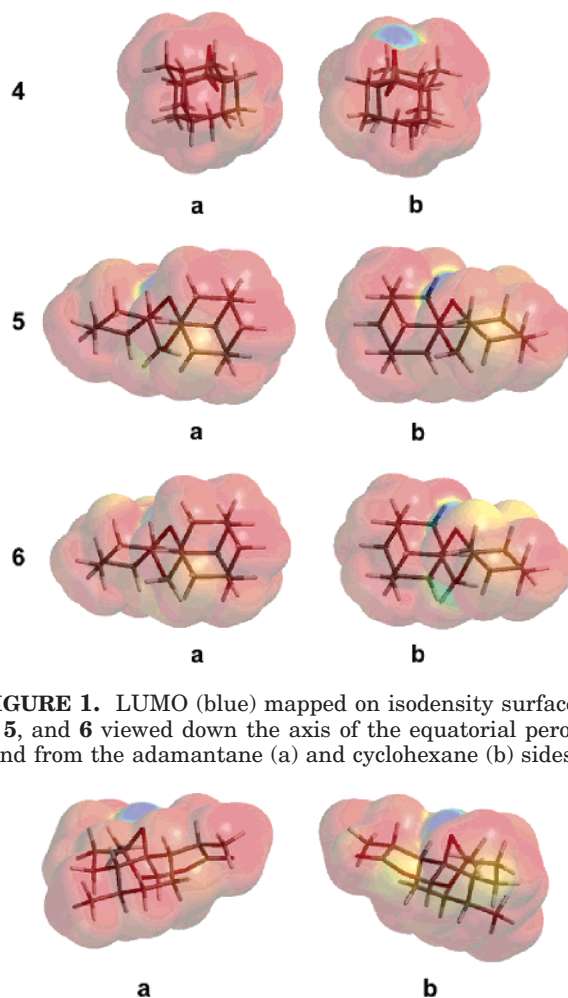


FIGURE 1. LUMO (blue) mapped on isodensity surfaces of **4**, **5**, and **6** viewed down the axis of the equatorial peroxide bond from the adamantane (a) and cyclohexane (b) sides.

FIGURE 2. LUMO (blue) mapped on the isodensity surface of **1** viewed down the axis of the peroxide bond from the O^1 (a) and O^2 (b) direction.

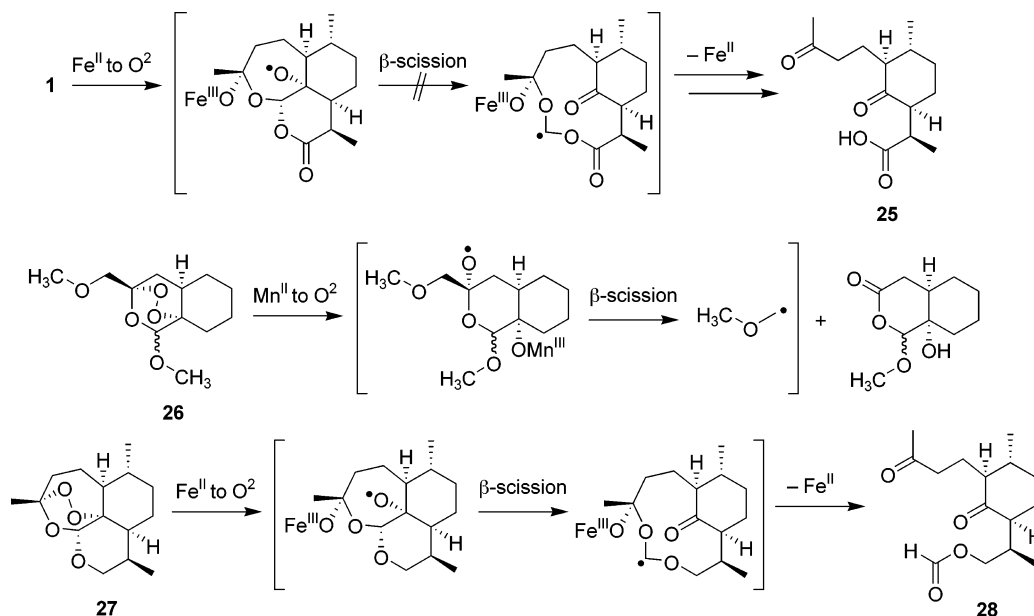
planes of the adamantane and cyclohexane rings can be calculated; for **4** it is 214° , whereas for **5** and **6** it is 167° .

The less exposed and presumably more biologically stable peroxide bonds in **5** and **6** vs **1** and **4** (Figures 1 and 2) may explain why the two trioxanes are so much less active than **1** or their trioxolane chemical cousin **4**, although the release of ring strain with peroxide bond cleavage in the six-membered 1,2,4-trioxane **1** is less than that for the five-membered 1,2,4-trioxolane **4**. Another contributing factor could be that **5** and **6**, unlike **1** and **4**, undergo reaction pathways to form relatively stable α -oxa primary carbon-centered radicals that unravel to carbonyl-containing end products. The latter, unlike carbon-centered radicals, presumably contribute little to their antimalarial properties. In this regard, it is notable that **6**, the trioxane completely devoid of antimalarial activity, also produced the largest proportion of carbonyl-containing end products and the lowest proportion of carbon-centered radicals. Consistent with this, **1** does not undergo β -scission pathway c (Scheme 1) that would form the stabilized α -dioxa (methylenedioxy) carbon-centered radical, as evidenced by the absence of the expected diketoacid end product **25** (Scheme 7). A complementary example is provided by synthetic trioxane **26**³⁷ that undergoes exclusive β -scission to form an α -oxa primary

(35) Walling, C.; Padwa, A. *J. Am. Chem. Soc.* **1963**, *85*, 1593–1597.

(36) Conformational analysis of **4–6** using MMFF94 with the Monte Carlo method revealed that the chair conformations of the cyclohexane rings in **4–6** are the most stable conformations. Also, in both the trioxolane and trioxane rings there exist two stable conformations of the same energy. The four stable conformations of each compound were subjected to ab initio geometry optimizations via HF/6-31G*. Again, the trioxolane and trioxane rings were found to have two equal energy conformations. Consequently, only two conformations of the cyclohexane ring where the peroxide linkage was in either the axial or equatorial positions were considered.

SCHEME 7



carbon-centered radical; as predicted, this trioxane is inactive. The foregoing, however, does not provide a satisfactory explanation for the 4-fold greater potency of deoxoartemisinin (**27**) vs that of **1**,³⁸ as the major iron(II) reaction product of the former is diketo formate ester **28**³⁹ produced by a putative β-scission pathway^{2b} that we suggest proceeds by way of an α-dioxa (methylenedioxy) carbon-centered radical.⁴⁰ Derivatives of **27** seem to fragment by this same pathway to afford carbonyl-containing end products.⁴¹

Although this study did not provide definitive answers to whether the primary or secondary carbon-centered radicals or a combination of the two contribute to the antimalarial activity of **1**, the results did suggest a small preference for attack of Fe(II) on the nonketal peroxide oxygen atom (O¹) of **1**.⁴² In addition, the iron(II) fragmentation of **4** clearly demonstrates that a peroxide need not fragment to form a primary carbon-centered radical to be active. Nevertheless, **1** alkylates free heme⁵ or hemoglobin heme⁴³ by way of the primary carbon-centered radical (O¹ pathway), possibly the only malaria-

parasite-relevant fully characterized alkylation reactions so far reported for **1**.

Experimental Section

Adamantane-2-spiro-3'-1',2',4'-trioxaspiro[5.5]undecane (5). *p*-Toluenesulfonic acid monohydrate (40 mg, 0.2 mmol) was added to a mixture of **10**¹² (280 mg, 1.9 mmol), 2-adamantanone (450 mg, 3 mmol), CH₂Cl₂ (10 mL) and 1,2-dichloroethane (10 mL). The reaction mixture was stirred at room temperature overnight, washed with saturated NaHCO₃ (15 mL), water (15 mL) and brine (15 mL), dried over MgSO₄, filtered and concentrated. The crude product was purified by flash chromatography using gradient elution (sg, 2–4% ether in hexane) to afford **5** as a colorless solid (500 mg, 95%). Mp 45–48 °C (ethanol/H₂O 2:1); ¹H NMR δ 1.22–2.05 (m, 22H), 2.37 (brs, 1H), 2.95 (brs, 1H), 3.51 (brs, 1H), 3.69 (brs, 1H); ¹³C NMR δ 21.4, 25.9, 27.17, 27.19, 28.5, 30.2, 32.3, 33.3, 33.4, 36.2, 37.2, 65.3, 77.3, 104.2. Anal. Calcd for C₁₇H₂₆O₃: C, 73.34; H, 9.41. Found: C, 73.50; H, 9.21.

Adamantane-2-spiro-3'-1',2',5'-trioxaspiro[5.5]undecane (6). 10-Camphorsulfonic acid (80 mg, 0.35 mmol) was added to a mixture of **11** (680 mg, 3.5 mmol), cyclohexanone (686 mg, 7.0 mmol) and CH₂Cl₂ (30 mL). The reaction mixture was stirred at room temperature overnight, washed with saturated NaHCO₃ (30 mL), water (30 mL), and brine (30 mL), dried over MgSO₄, filtered and concentrated. The crude product was crystallized from 80% aqueous ethanol to afford **6** as a colorless solid (740 mg, 76%). Mp 85–87 °C (80% aqueous ethanol); ¹H NMR δ 1.40–2.36 (m, 23H), 2.73 (brs, 1H), 3.71 (brs, 1H), 4.05 (brs, 1H); ¹³C NMR δ 22.4, 25.6, 27.4, 27.5, 28.6, 29.3, 32.0, 33.6, 34.2, 37.8, 63.6, 81.1, 101.9. Anal. Calcd for C₁₇H₂₆O₃: C, 73.34; H, 9.41. Found: C, 73.49; H, 9.48.

7-(4-Oxo-2,2,6,6-tetramethyl-1-piperidinyloxy)bicyclo-[3.3.1]nonane-3-carboxylic acid (22). To a solution of **4** (264 mg, 1.0 mmol), 4-oxo-TEMPO (340 mg, 2.0 mmol) in CH₂Cl₂ (10 mL) and CH₃CN (10 mL) was added Fe(OAc)₂ (261 mg, 1.5 mmol). The resulting mixture was stirred under N₂ and 35 °C for 24 h before being quenched with water (50 mL) and acetic acid (3 mL). After separation of the organic layer, the aqueous layer was extracted with CH₂Cl₂ (2 × 20 mL). The combined extracts were washed with brine (2 × 30 mL), dried over MgSO₄, filtered and concentrated. The crude product was purified by flash chromatography using gradient elution (sg,

(37) Cazelles, J.; Camuzet-Dedenis, B.; Provot, O.; Robert, A.; Mayrargue, J.; Meunier, B. *J. Chem. Soc., Perkin Trans. 1* **2000**, 1265–1270.

(38) Jung, M.; Li, X.; Bustos, D. A.; ElSohly, H. N.; McChesney, J. D.; Milhous, W. K. *J. Med. Chem.* **1990**, *33*, 1516–1518.

(39) Avery, M. A.; Fan P.; Karle, J. M.; Bonk, J. D.; Miller, R.; Goins, D. K. *J. Med. Chem.* **1996**, *39*, 1885–1897.

(40) Alternate pathways (refs 10 and 39) to account for the formation of **28** from **27** have been proposed.

(41) O'Neill, P. M.; Pugh, M.; Stachulski, A. V.; Ward, S. A.; Davies, J.; Park, B. K. *J. Chem. Soc., Perkin Trans. 1* **2001**, 2682–2689.

(42) As one reviewer pointed out, it is interesting to note that epiartemisinin (C9 α-epimer), with its more sterically hindered inner peroxide oxygen atom (O¹), is 1.5- to 7-fold less potent than **1**. This activity difference was rationalized in terms of a preferential attack of Fe(II) (heme) at the outer peroxide oxygen atom (O²) of epiartemisinin to give mainly the secondary carbon-centered radical. (a) Acton, N.; Klayman, D. L. *Planta Med.* **1987**, *266*–268. (b) Avery, M. A.; Gao, F.; Chong, W. K. M.; Mehrotra, S.; Milhous, W. K. *J. Med. Chem.* **1993**, *36*, 4264–4215. (c) Jefford, C. W.; Burger, U.; Millasson-Schmidt, P.; Bernardinelli, G.; Robinson, B. L.; Peters, W. *Helv. Chim. Acta* **2000**, *83*, 1239–1246.

(43) Selmecezi, K.; Robert, A.; Claparols, C.; Meunier, B. *FEBS Lett.* **2004**, *556*, 245–248.

10–90% EtOAc in hexane) to give 2-adamantanone (8 mg, 5%), **14** (46 mg, 28%), **16**²³ (10 mg, 6%), and **22** (190 mg, 56%) as a colorless solid. For **22**: mp 179–180 °C (ether/hexane 1:3); ¹H NMR δ 1.14 (s, 6H), 1.14–1.18 (m, 1H), 1.24–1.35 (m, 3H), 1.30 (s, 6H), 1.50–1.61 (m, 3H), 2.08–2.30 (m, 7H), 2.48–2.62 (m, 3H), 4.04–4.13 (m, 1H); ¹³C NMR δ 22.7, 26.0, 28.7, 29.2, 33.8, 35.4, 39.5, 53.5, 62.8, 76.1, 181.7, 208.6. HRMS-FAB for C₁₉H₃₁NO₄ [M + H]⁺: calcd 338.2253, found 338.2321.

(1-Hydroxycyclohexyl)methyl 7-(4-Oxo-2,2,6,6-tetramethyl-1-piperidinyloxy)-bicyclo[3.3.1]nonane-3-carboxylate (23). A mixture of **5** (240 mg, 0.86 mmol), FeBr₂ (370 mg, 1.72 mmol), 4-oxo-TEMPO (294 mg, 1.72 mmol) and THF (10 mL) was stirred at ambient temperature under a N₂ atmosphere for 16 h and concentrated. The crude product was dissolved in EtOAc, washed with water and brine, dried over MgSO₄, filtered and concentrated. The crude product was purified by flash chromatography using gradient elution (sg, 10–60% EtOAc in hexane) to afford **23** (220 mg, 57%) as a colorless oil (single isomer). ¹H NMR δ 1.12 (s, 6H), 1.10–1.18 (m, 1H), 1.28 (s, 6H), 1.24–1.34 (m, 4H), 1.40–1.68 (m, 12H), 1.85 (brs, 1H, OH), 2.08–2.30 (m, 8H), 2.52–2.60 (m, 2H), 3.98 (s, 2H), 4.04–4.11 (m, 1H); ¹³C NMR δ 21.5, 22.6, 25.6, 25.9, 28.4, 29.4, 33.9, 34.3, 35.6, 39.5, 53.5, 62.6, 70.5, 71.3, 76.1, 176.5, 208.6. HRMS-FAB for C₂₆H₄₄NO₅ [M + H]⁺: calcd 450.3219, found 450.3210.

(2-Hydroxy-2-adamantyl)methyl 6-(4-Oxo-2,2,6,6-tetramethyl-1-piperidinyloxy)hexanoate (24). A mixture of **6** (240 mg, 0.86 mmol), FeBr₂ (370 mg, 1.72 mmol), 4-oxo-TEMPO (294 mg, 1.72 mmol) and THF (10 mL) was stirred at ambient temperature under a N₂ atmosphere for 30 h and concentrated. The crude product was dissolved in EtOAc,

washed with water and brine, dried over MgSO₄, filtered and concentrated. The crude product was purified by flash chromatography using gradient elution (sg, 10–50% EtOAc in hexane) to give 2-adamantanone (50 mg, 39%) and **24** (85 mg, 22%) as a colorless oil. ¹H NMR δ 1.15 (s, 6H), 1.28 (s, 6H), 1.40–1.46 (m, 2H), 1.52–1.87 (m, 16H), 2.05 (brs, 1H, OH), 2.20 (d, *J* = 12.7 Hz, 2H), 2.23 (d, *J* = 15.6 Hz, 2H), 2.39 (t, *J* = 7.4 Hz, 2H), 2.55 (d, *J* = 12.7 Hz, 2H), 3.82 (t, *J* = 6.4 Hz, 2H), 4.29 (s, 2H); ¹³C NMR δ 22.5, 25.1, 26.0, 27.0, 27.4, 28.3, 32.4, 32.5, 34.2, 34.4, 34.6, 38.0, 53.5, 62.9, 68.9, 74.0, 76.7, 173.8, 208.3. HRMS-FAB for C₂₆H₄₄NO₅ [M + H]⁺: calcd 450.3219, found 450.3221.

Acknowledgment. We thank the Medicines for Malaria Venture (MMV) for generous support of this research and Reto Brun and Sergio Wittlin of the Swiss Tropical Institute for the antimalarial data of **1**, and **4–7**. We acknowledge the Nebraska Center for Mass Spectrometry for the HRMS data.

Supporting Information Available: Alternate synthesis of **5** and synthesis and characterization data for **7–21**, *O*-benzyl oxime synthesis and quantitation, antimalarial assays, computational chemistry methods, ¹³C NMR spectra for compounds **18a–d** and **19–24**, and total energies and atomic coordinates to support the M.M. and M.O. calculations. This material is available free of charge via the Internet at <http://pubs.acs.org>.

JO050385+